RC 22515 (W0207-052) July 12, 2002
Materials Science

IBM Research Report

High-resolution x-ray diffractionfor characterization and monitoring of silicon-on-insulator fabrication processes

Guy M. Cohen, Patricia M. Mooney, H Park, Cyril Cabral Jr, Erin C. Jones
IBM Research Division
Thomas J. Watson Research Center
P.O. Box 218
Yorktown Heights, NY 10598

Research Division
Almaden - Austin - Beijing - Delhi - Haifa - India - T. J. Watson - Tokyo - Zurich

LIMITED DISTRIBUTION NOTICE: This report has been submitted for publication outside of IBM and will probably be copyrighted if accepted for publication. It has been issued as a Research Report for early dissemination of its contents. In view of the transfer of copyright to the outside publisher, its distribution outside of IBM prior to publication should be limited to peer communications and specific requests. After outside publication, requests should be filled only by reprints or legally obtained copies of the article (e.g. , payment of royalties). Copies may be requested from IBM T. J. Watson Research Center , P. O. Box 218, Yorktown Heights, NY 10598 USA (email: reports@us.ibm.com). Some reports are available on the internet at http://domino.watson.ibm.com/library/CyberDig.nsf/home .

High-resolution x-ray diffraction for characterization and monitoring of silicon-on-insulator fabrication processes

G. M. Cohen, P.M. Mooney, H. Park, C. Cabral, Jr., and E.C. Jones

IBM Research Division, T. J. Watson Research Center

P.O. Box 218, Yorktown Heights, NY 10598, U.S.A

Abstract

High-resolution x-ray diffraction (HRXRD) was used to monitor silicon-on-insulator (SOI) device fabrication processes. The use of HRXRD is attractive since it is non-destructive and can be applied directly to product wafers. We show the usefulness of this technique for the characterization of amorphizing implants for shallow junctions, solid phase re-crystallization of implanted junctions, cobalt-silicide formation, and oxidation; all are critical processes for complementary metal oxide semiconductor (CMOS) device fabrication on SOI. We also found the technique applicable to multi-layered SOI structures fabricated by wafer bonding, where the tilt and rotation of each SOI layer with respect to the handle substrate, allowed us to obtain independent measurements of each SOI film.

Introduction

Reducing the gate length of metal oxide semiconductor field effect transistor (MOSFET) built on SOI requires scaling the SOI film thickness [1,2]. Downscaling the gate-length without scaling the SOI film thickness would lead to a MOSFET having a threshold voltage which is gate-length dependent. This effect is also known as the short channel effect. Since some spread in the gate-length is expected in chip manufacturing, the effect may detrimental to circuit operation. By thinning the SOI film the dependency of the threshold voltage on the gate length is suppressed. However, manufacturing of MOSFET devices on thin SOI is challenging, since it requires a tighter control over most processes that modify the SOI film.

The idea behind the use of HRXRD to monitor SOI processing is straightforward. Oxidation, silicide formation and amorphizing implants reduce the single crystal SOI film thickness, which is easily and accurately measured by HRXRD [3]. For example, oxidation converts the upper part of the SOI film into SiO_2. Similarly, silicidation reacts a metal (such as Co) with the top portion of the SOI film to form a silicide (such as CoSi and $CoSi_2$). The phase of the silicide that is formed can be determined from the amount of Si consumed. In the case of amorphizing implants, which are routinely used to form the source and drain regions of a device [4], a portion of the SOI film is converted from single crystal silicon to amorphous silicon. Post-implant annealing, typically carried out by rapid thermal annealing (RTA), re-crystallizes the amorphous portion of the film and restores the SOI film thickness. Accurate measurement of the SOI film thickness is essential for tight monitoring of all these processes.

The change in the SOI layer thickness is not the only parameter obtained from HRXRD measurements. The HRXRD data of amorphizing and non-amorphizing Ge, Si or boron implanted wafers, is further used to extract the strain profile and the implant damage profile in the SOI film. Moreover, in the case of boron-implanted wafers a change in the sign of the strain is recorded when the boron assumes a substitutional site following the RTA anneal.

HRXRD characterization is also found to be a powerful technique when applied multi-layered SOI structures. Such structures are built for 3D integration of circuits, and for hybrid systems on a chip. An example of such a structure is a double-bonded SOI substrate having two stacks of buried oxide and SOI films. Diffraction maps of this type of structure provide the thickness, tilt, and rotation of each SOI layer with respect to the handle substrate. Since each of the bonded SOI films has a different orientation due to tilt and rotation, a direct measurement of the properties of each SOI film is obtained.

X-ray measurements

The x-ray diffraction measurements were carried out with a Philips materials research diffractometer (MRD), which is equipped with an asymmetrically cut four-crystal Ge(220) monochromator and mounted on a rotating Cu anode x-ray source. ω is the angle between the incident beam and the wafer surface and 2θ is the angle between the incident beam and the detector, i.e. the reflected beam; therefore the angle of the incident or reflected beam with respect to the analyzed atomic planes, the Bragg angle, is $\theta_B = 2\theta/2$. The angle ϕ denotes a rotation in

the plane of the wafer. The 004 reflection was measured in the triple-axis (TA) mode [5], i.e. by taking $\omega/2\theta$ scans with an analyzer crystal installed in front of the detector. The use of an analyzer crystal suppresses the background scattering, thus enhancing the thickness fringes. The 113 reflections were measured using a large detector aperture and standard rocking curves (ω scans). The 113 reflection, taken with a low angle incidence beam, is surface sensitive and thus is useful for the measurement of very thin films.

For the various experiments discussed in this paper, we used commercially available bonded wafers or separation by implanted oxygen (SIMOX) wafers. The multi-layered SOI wafers were prepared in our lab by transferring a silicon film onto a bonded SOI wafer having a thermal oxide film grown on the SOI film. The bond was formed between the silicon film and the thermal oxide film. An anneal at 1050°C was used to strengthen the bond. The film stack thus formed is illustrated in Fig. 1(a).

Results and Discussion

I. Multi-layered SOI

In a recent publication we have shown that the SOI film properties such as thickness, tilt, and rotation can be obtain by HRXRD [3]. In this paper we demonstrate experimentally that the same method can be applied to a multi-layer SOI structure. Figure 1(b) shows a ω-2θ diffraction map in which a double-bonded SOI substrate having two stacks of buried oxides and SOI films

was measured. The structure is illustrated in Fig.1(a). The diffraction peak associated with the substrate and the two peaks from the SOI films are measured at the same Bragg angle, confirming that there is no strain the in the SOI films. The thickness of each SOI layer is readily extracted from the side-lobe spacing. Due to unintentional wafer miscut, the lattice planes in the bonded SOI films and the handle Si substrate are slightly tilted with respect to each other. Therefore the diffraction peaks from the Si substrate and each SOI layer appear at different incident angles (ω). This makes it possible to measure each of the SOI films in the stack independently [3]. The independent measurement of each SOI film in the stack is an important advantage of HRXRD over common methods such as ellipsometry and reflectometry, where a spatial separation of signals associated with different layers in the film stack does not exist. Additionally, HRXRD is blind to non-crystalline films thus further simplifying the analysis of a multi-layered SOI stack, which typically contains amorphous layers such as a buried oxide layer. We further note that in most practical cases the measurement of a diffraction map is not necessary since most of the film properties can be obtained by taking a single ω-2θ line scan at the ω corresponding to that film.

II. Silicidation

Figure 2 demonstrates how the cobalt silicide formation process is monitored on an SOI wafer. The process begins with the sputter deposition of a 6 nm thick cobalt layer over the SOI film. The cobalt layer is capped with a 20 nm thick TiN film to prevent the cobalt from oxidizing during annealing. A first anneal at a temperature of 520°C is performed to react all the cobalt with the underlying silicon to form the mono-silicide phase, CoSi. The TiN cap and unreacted

cobalt on the regions of the wafer having no exposed Si (e.g. dielectric isolation regions) are then selectively etched off, and a second anneal at a temperature of 750°C is performed to form the disilicide phase, $CoSi_2$. Since the silicide reaction is self-limited, the nominal amount of silicon consumed from the SOI layer is known. The formation of the CoSi phase requires 1.82 nm of silicon per 1 nm of metal and the formation of the $CoSi_2$ phase takes 3.64 nm of silicon for each nanometer of metal [6]. By monitoring the change in the SOI thickness, which is equivalent to the amount of silicon reacted to form the silicide, it is possible to confirm the formation of the desired silicide phases.

To minimize the parasitic resistance of high-speed devices it is critical to form the lowest resistivity silicide phase. The $CoSi_2$ phase is used, since it exhibits a lower sheet resistance than CoSi. The lowest resistivity phase is not always the disilicide phase, however. For example, nickel mono-silicide (NiSi) has a lower resistivity than the disilicide $NiSi_2$.

Figure 2(a) shows a 004 triple-axis scan of the as-deposited cobalt on a bonded SOI wafer, where the diffraction peak of the SOI layer is offset from that of the substrate [3]. The trace is recorded with the incident angle, ω, centered at the SOI layer diffraction peak. The SOI layer thickness is accurately measured from the period of the thickness fringes (also known as Pendellosung fringes). Figure 2(b) shows a scan following the first anneal which forms the monosilicide phase, and Fig. 2(c) shows a scan following the second anneal which forms the disilicide phase. As is clearly seen, the fringe spacing increases when the silicide phase becomes more silicon rich. By measuring the change in the SOI thickness the silicide phase is identified as indicated on figures 2(b) and 2(c). The initial SOI film thickness on which 6 nm of Co were

deposited was 96 nm. After the formation of the CoSi phase the SOI film measured 87 nm and following the formation of the $CoSi_2$ phase it was further reduced to 74 nm. Using the literature data for the amount of silicon required to form a Co-silicide [6], SOI film thicknesses are expected to be 85.1 and 74.6 nm respectively. The accuracy in the determination of the amount of consumed Si will increase as future CMOS technology migrates to thinner SOI films, since the absolute error in the film thickness measurement is smaller for thinner films.

III. Ion Implantation

Ion implantation is another key process for semiconductor device fabrication. To obtain a shallow junction by implanting a light atom dopant such as boron, a pre-amorphizing implant of Ge is used. The amorphized surface layer prevents boron channeling, which would lead to a tail in the boron profile. The thickness of the amorphized portion of the SOI film is easily obtained by measuring the thickness of the remaining crystalline portion of the film.

To investigate amorphizing implants by HRXRD we implanted Ge into a SIMOX wafer using different implant conditions. For SIMOX wafers, the lattice planes of the SOI layer have the same orientation as those of the Si substrate and therefore the diffraction peak from the SOI layer overlaps that from the Si substrate. Figure 3 shows three rocking curves that correspond to the initial SOI wafer and two different implant conditions. The first trace (solid line) of figure 3 is a measurement of a region with no implant. The second trace (dashed line) corresponds to a Ge dose of $3x10^{14}$ cm^{-2} and implant energy of 15 keV, and the third trace (dash-dot line) corresponds to an implant with the same dose but a higher energy of 30 keV. The implanted

samples show a larger fringe spacing than of the non-implanted sample, because the top portion of the single crystal SOI film was amorphized. The traces from the implanted samples also show an asymmetric spectrum, having pronounced thickness oscillations for negative ω and few attenuated fringes for positive ω. This asymmetry is due to the strain and damage introduced by the implant into the crystalline portion of the SOI, as explained below.

Cross-sectional transmission electron microscope (TEM) images (Fig. 4) confirm that the top portion of the SOI film is amorphized by the implant. A 15 keV implant resulted in a 20.5 nm thick amorphous layer, while the 30 keV-implant amorphized about 37.2 nm of single crystal silicon. These layer thicknesses are the same as those determined from the HRXRD measurements of Fig. 3. In general we found that the measured SOI film thickness obtained with HRXRD agreed within 1% with the thickness found from TEM cross-sections of the same sample.

Figure 5 shows the rocking curve from a SOI film implanted with a Ge dose of $3x10^{13}$ cm^{-2} at an energy of 50 keV, and Fig. 6 shows a TEM cross-section of the same sample. Due to the lower Ge dose, this implant does not amorphize the SOI film. Hence the fringe spacing is the same as that of the unmplanted SIMOX sample. To explain the asymmetry in the rocking curve, we simulated the diffraction pattern using the wave summation approach outlined in Ref 7. The Ge implant leads to compressive strain and damage in the SOI film. There were both incorporated into the simulation by sectioning the SOI layer into N laminae, each described by two parameters to represent the strain and the static atomic disorder. The strain distribution is represented by a set of coherently diffracting laminae. The laminae all have the same in-plane

lattice parameter, but the out-of-plane lattice parameter of each one varies according to an assigned uniform strain value chosen to approximate the strain profile introduced by the implant. In addition to the coherent atomic displacements (strain), static random displacements (damage) are treated through their effect on the mean structure factor in each lamina [8]. The static atomic displacement factor is also known as the Debye-Waller factor, which accounts for the displacements of atoms from their lattice position. The higher the static atomic disorder value assigned to a lamina the less diffractive the lamina.

We further assumed that a sum of Gaussian distributions could approximate the strain and damage profiles. Both the center position and width of each distribution were varied independently to obtain the best fit with the measured data. The strain profile and damage profiles giving the best simulation are shown in Fig. 7. The maximum positions of the strain distribution and of the atomic disorder distribution obtained from simulation are in excellent agreement with the position of the maximum damage found by TEM. The simulated rocking curve, shown in Fig. 5, predicts well all the features in the measured rocking curve. We note that the measured intensity is greater than the calculated intensity away from the center of the scan because of the high background scattering measured when data are taken without a receiving slit or analyzing crystal to reduce the detector aperture. The simulation can be improved by not fixing the distributions to an analytical form (such as the Gaussian distribution we used), but rather allowing the distribution to be calculated using a minimization procedure as discussed in [9].

The same simulation approach can be used to calculate the rocking curve in the case of an amorphizing implant. As an example, Fig. 8 shows the calculated and measured 113 rocking curves of the SOI film implanted with an amorphizing Ge dose of $3x10^{14}$ cm^{-2} and energy of 30 keV. A good fit is obtained when the top amorphized portion of the SOI film is set as non-diffracting, and the damaged and strained distributions assume their maximum values at the silicon to amorphous silicon interface. To account for the high background scattering we added a constant number to the simulated curve. The TEM image of the implanted sample (Fig. 4(c)) confirms that the top portion of the SOI film is amorphized and there is a damaged single-crystal region below the amorphized portion of the SOI film. We note that the damping out of the fringes at positive ω is accounted for primarily by the inclusion of damage in the simulation.

Figures 9 and 10 demonstrate how HRXRD can be used to monitor RTA processing of implanted wafers. Figure 9 shows the rocking curves of a SIMOX sample that was implanted with a Si dose of $5x10^{14}$ cm^{-2} and energy of 23.8 keV and then annealed at 1000 °C for 2 seconds by RTA. The rocking curve clearly shows that the Si implant amorphized the top portion of the SOI film, and induces damage which cause the film to be strained compressively, similarly to what occurs for the Ge implants. During RTA the amorphous silicon film re-crystallizes by solid phase epitaxy and the thickness fringe spacing is restored to its pre-implant value (shown in figure 3 by the solid line). The post-RTA curve shows a slight asymmetry, which is due to residual damage that was not removed by RTA.

Figure 10 shows the rocking curve of a sample that was implanted with a boron dose of $3x10^{14}$ cm^{-2} and energy of 3.8 keV. The thickness fringe spacing does not change since the light-

mass boron atom does not amorphize the film. The rocking curve indicates that the post-implanted film is compressively strained, due to implant damage and the boron mostly assuming interstitial sites. As is seen from the layer peak shift, following an anneal at 1000 °C for 2 seconds by RTA, the boron atoms assume substitutional sites and the strain in the SOI film becomes tensile, since boron is a smaller atom than silicon.

Conclusions

We have demonstrated that HRXRD can be used to monitor critical SOI device fabrication steps. This technique is non-destructive and can, therefore, be applied to product wafers. While these measurements primarily provide the thickness change in the SOI film due to device fabrication processes, additional information such as the ion implantation damage and the strain distribution in the film was also obtained by simulating the x-ray diffraction data. The method was also applied to multi-layered bonded SOI substrates, and is shown to be advantageous compared to commonly used optical techniques due to its ability to provide independent measurements of each SOI layer.

References:

1. L. T. Su, J. B. Jacobs, J. E. Chung, D. A. Antoniadis, IEEE Electron Device Lett. **15**, 366 (1994).

2. H-S. P. Wong, D. J. Frank, and P. M. Solomon, IEDM Technical digest, p. 407, (1998).

3. G. M. Cohen, P. M. Mooney, E. C. Jones, K. K. Chan, P. M. Solomon, and H-S. P. Wong, Appl. Phys. Lett., **75**(6), 787, (1999).

4. S. Wolf and R. N. Tauber, *Silicon Processing for the VLSI Era*, Vol. 1, Lattice Press, Sunset Beach, CA, (1986).

5. P.F. Fewster, Semicond. Sci. Technol. **8**, 1915 (1993).

6. S. P. Murarka, Silicides for VLSI Applications, Academic Press New York, 1983.

7. E. Zolotoyabko, J. Appl. Cryst. **31,** 241 (1998).

8. V. S. Speriosu, J. Appl. Phys. **52**(10), 6094, (1981).

9. A. Parisini, S. Milita, and M. Servidori, Acta Cryst. **A52**, 302, (1996).

Figure captions:

Fig. 1. (a) An 004 triple-axis ω-2θ diffraction map measured for a double-bonded two-layer SOI on silicon substrate. The measured SOI film thicknesses are 65 nm and 133 nm as obtained from the thickness fringes spacing. (b) Diagram of a double-bonded SOI substrate having two buried oxide layers and two SOI layers. The orientation of the lattice planes is shown schematically.

Fig. 2. An 004 triple-axis scan of a bonded SOI wafer, showing only the diffraction pattern obtained from the SOI film. (a) With as deposited cobalt. (b) After first RTA that forms cobalt monosilicide. (c) After second anneal that form the cobalt disilicide. SOI layer thicknesses obtained from simulations are 96, 87, and 74 nm.

Fig. 3. 113 rocking curves of a SIMOX wafer. The solid line is a measurement of a region with no implant. The dashed line corresponds to a Ge dose of $3x10^{14}$ cm^{-2} and implant energy of 15 keV, and the dash-dot line corresponds to an implant with the same dose but a higher energy of 30 keV. SOI layer thicknesses obtained from simulations are 122.4, 102, and 86 nm.

Fig. 4. TEM images corresponding to the measurements shown in Fig 3. (a) A region with no implant.(b) A region implanted with a Ge dose of $3x10^{14}$ cm^{-2} and implant energy of 15 keV. (c) An implant region with the same dose but a higher energy of 30 keV.

Fig. 5. A 113 rocking curve of a SOI film (shown in Fig.6) implanted with a Ge dose of $3x10^{13}$ cm^{-2} and energy of 50 keV (solid line). The open circles show a simulation obtained by fitting the strain and damage distribution in the film. The thickness of the SOI film obtained from simulation is 122.4 nm.

Fig. 6. A TEM image of a SOI film implanted with a Ge dose of $3x10^{13}$ cm^{-2} and energy of 50 keV. Note the implant damage.

Fig. 7. Strain and damage profile determined from the simulation of the SOI layer implanted with a Ge dose of $3x10^{13}$ cm^{-2} and energy of 50 keV.

Fig. 8. The measured (solid line) and simulated (open circles) 113 rocking curves of an SOI film implanted with an amorphizing Ge dose of $3x10^{14}$ cm^{-2} and energy of 30 keV. A TEM cross-section of this sample is shown in Fig.4(c). The thickness of the crystalline portion of the SOI film obtained from simulation is 86 nm.

Fig. 9. 113 rocking curves of a SIMOX sample that was implanted with a Si dose of $5x10^{14}$ cm^{-2} and energy of 23.8 keV (dashed line) and then annealed at 1000 °C for 2 seconds by RTA (solid line).

Fig. 10. 113 rocking curves of a sample that was implanted with a boron dose of $3x10^{14}$ cm^{-2} and energy of 3.8 keV (dashed line) and then annealed at 1000 °C for 2 seconds by RTA (solid line).

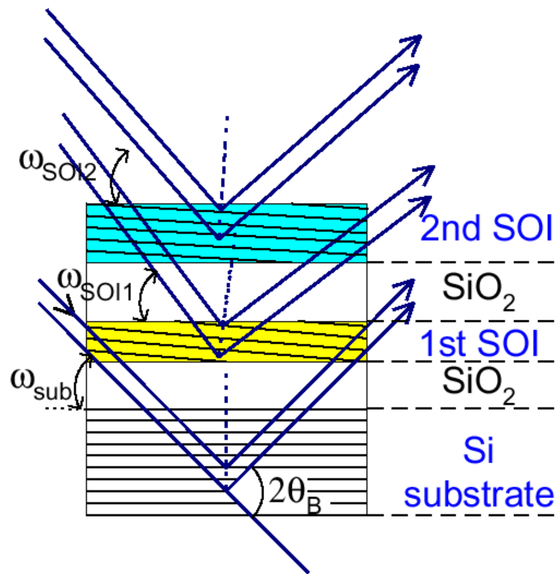

Figure 1(a): Cohen et al.

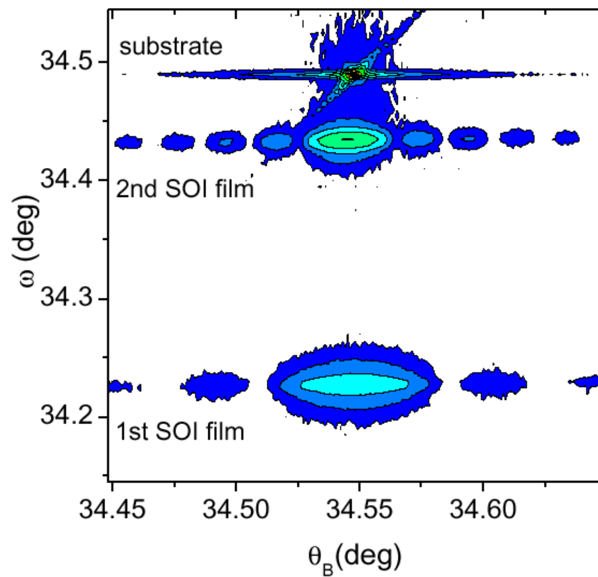

Figure 1(b): Cohen et al.

Fig. 1. (a) An 004 triple-axis ω-2θ diffraction map measured for a double-bonded two-layer SOI on silicon substrate. The measured SOI film thicknesses are 65 nm and 133 nm as obtained from the thickness fringes spacing. (b) Diagram of a double-bonded SOI substrate having two buried oxide layers and two SOI layers. The orientation of the lattice planes is shown schematically.

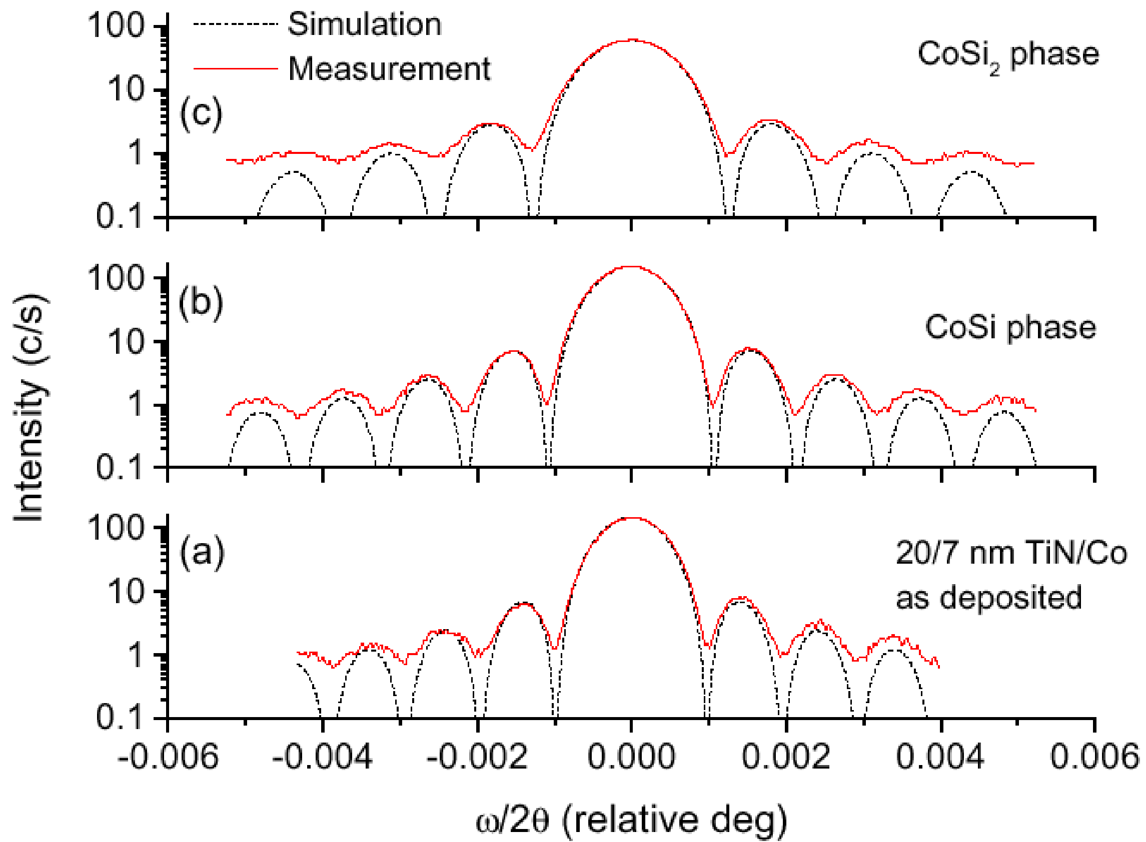

Fig. 2. An 004 triple-axis scan of a bonded SOI wafer, showing only the diffraction pattern obtained from the SOI film. (a) With as deposited cobalt. (b) After first RTA that forms cobalt monosilicide. (c) After second anneal that form the cobalt disilicide. SOI layer thicknesses obtained from simulations are 96, 87, and 74 nm.

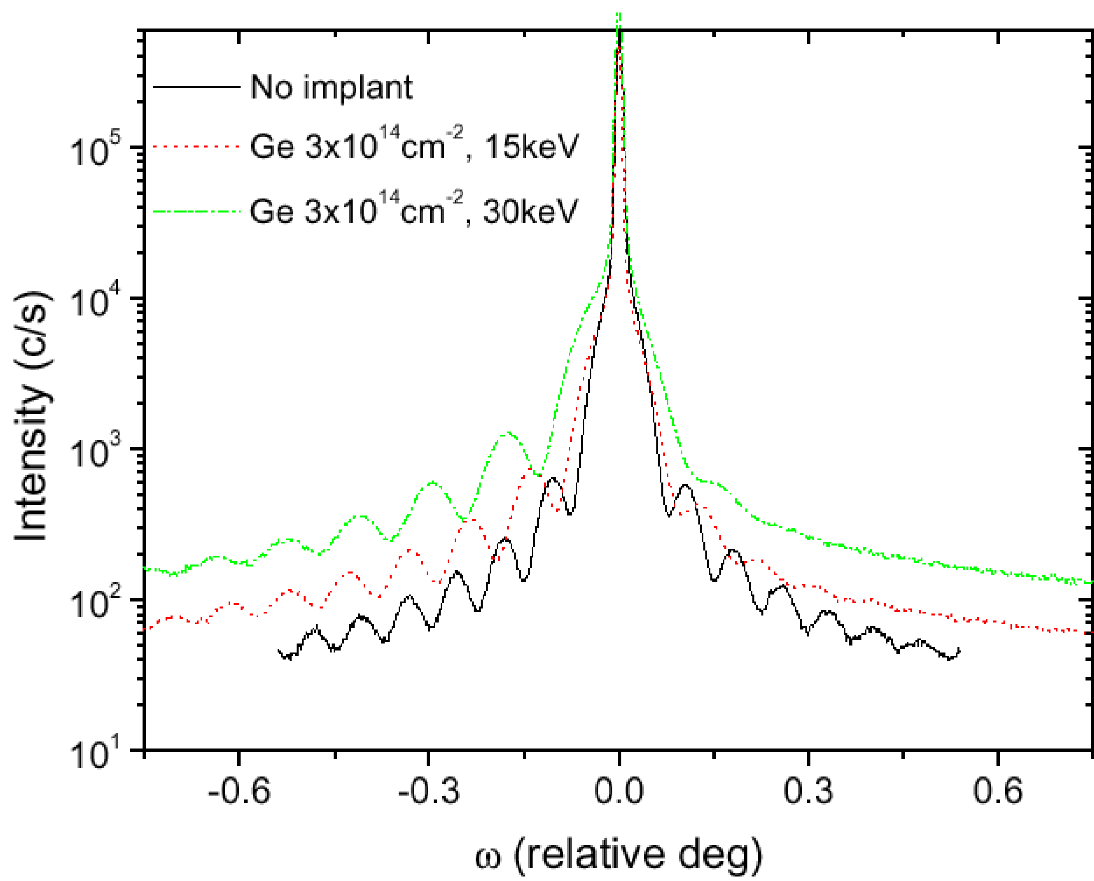

Fig. 3. 113 rocking curves of a SIMOX wafer. The solid line is a measurement of a region with no implant. The dashed line corresponds to a Ge dose of $3x10^{14}$ cm^{-2} and implant energy of 15 keV, and the dash-dot line corresponds to an implant with the same dose but a higher energy of 30 keV. SOI layer thicknesses obtained from simulations are 122.4, 102, and 86 nm.

\

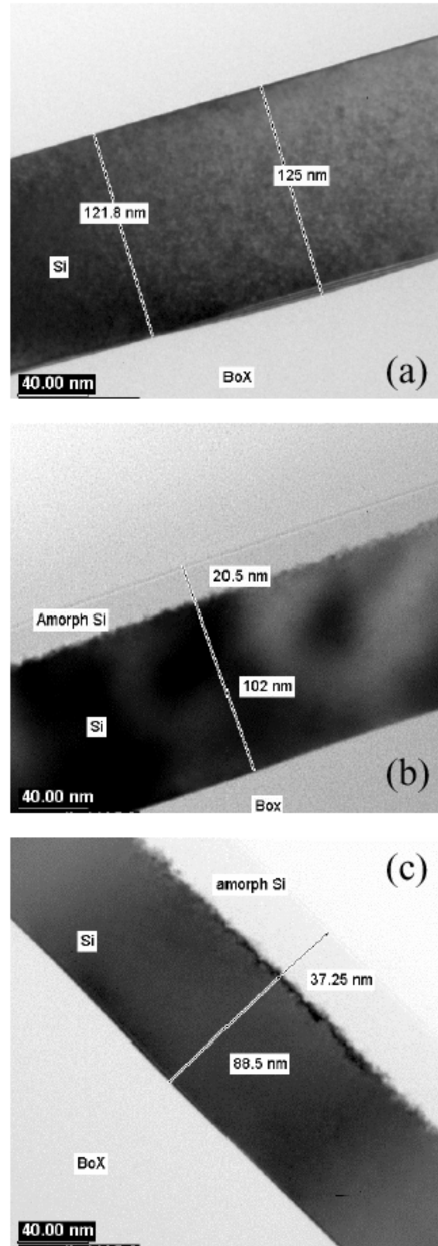

Figure 4: Cohen et al.

Fig. 4. TEM images corresponding to the measurements shown in Fig 3. (a) A region with no implant.(b) A region implanted with a Ge dose of $3x10^{14}$ cm^{-2} and implant energy of 15 keV. (c) An implant region with the same dose but a higher energy of 30 keV.

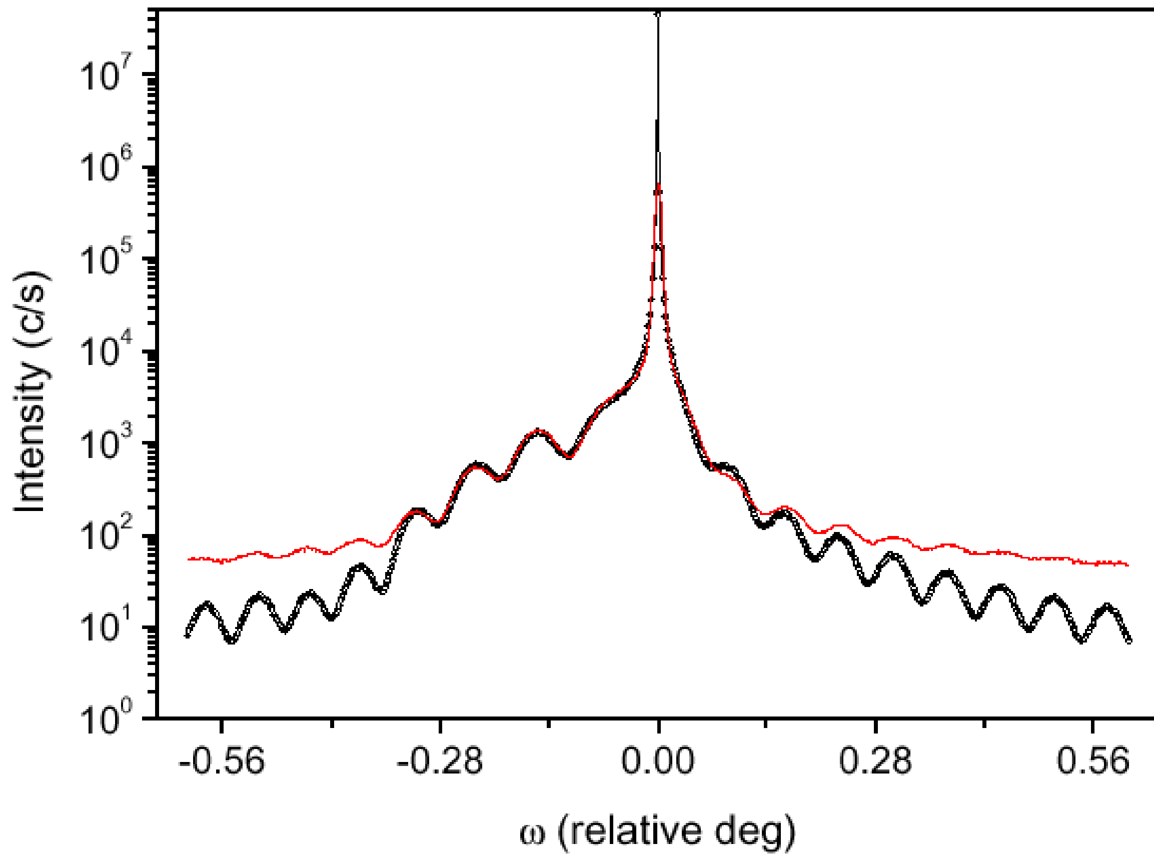

Figure 5: Cohen et al.

Fig. 5. A 113 rocking curve of a SOI film (shown in Fig.6) implanted with a Ge dose of $3x10^{13}$ cm^{-2} and energy of 50 keV (solid line). The open circles show a simulation obtained by fitting the strain and damage distribution in the film. The thickness of the SOI film obtained from simulation is 122.4 nm.

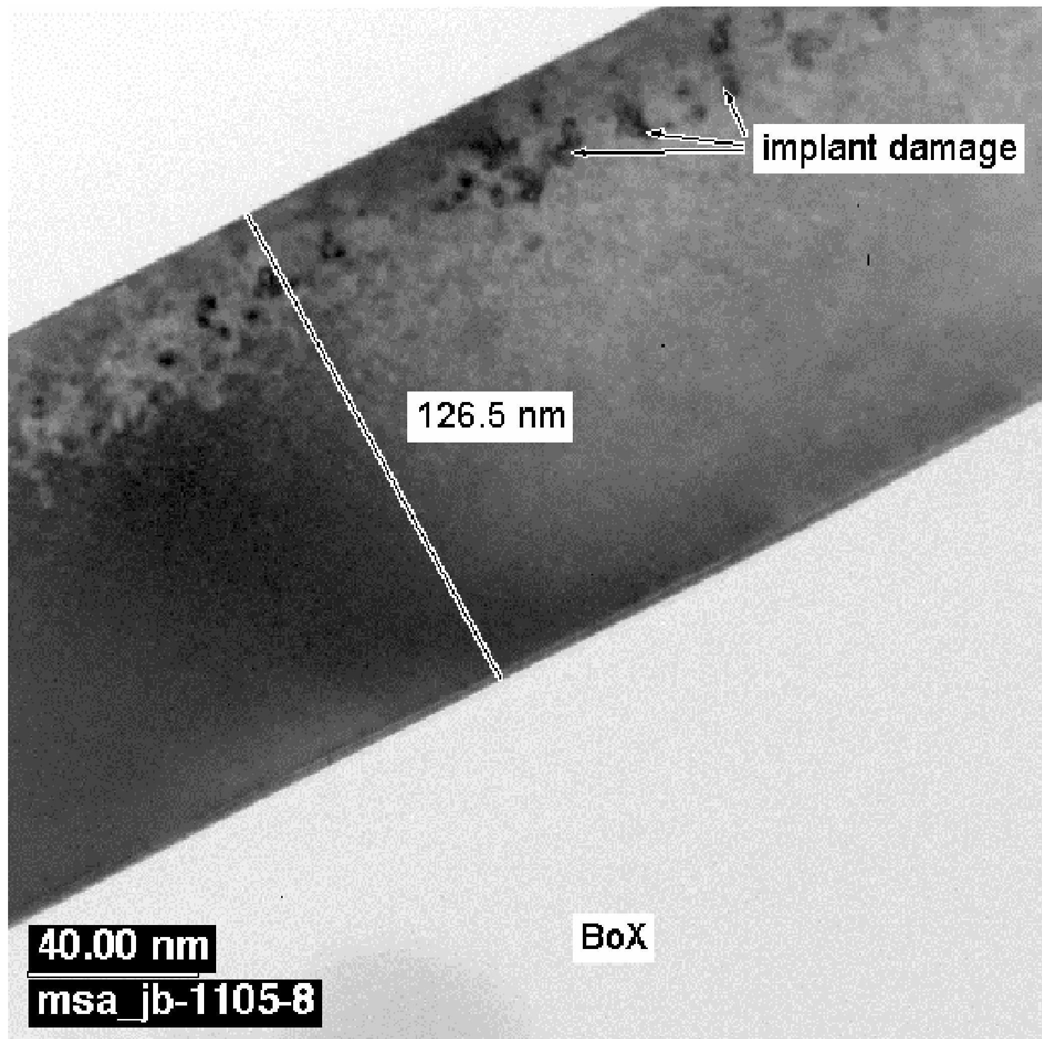

Figure 6: Cohen et al.

Fig. 6. A TEM image of a SOI film implanted with a Ge dose of $3x10^{13}$ cm^{-2} and energy of 50 keV. Note the implant damage.

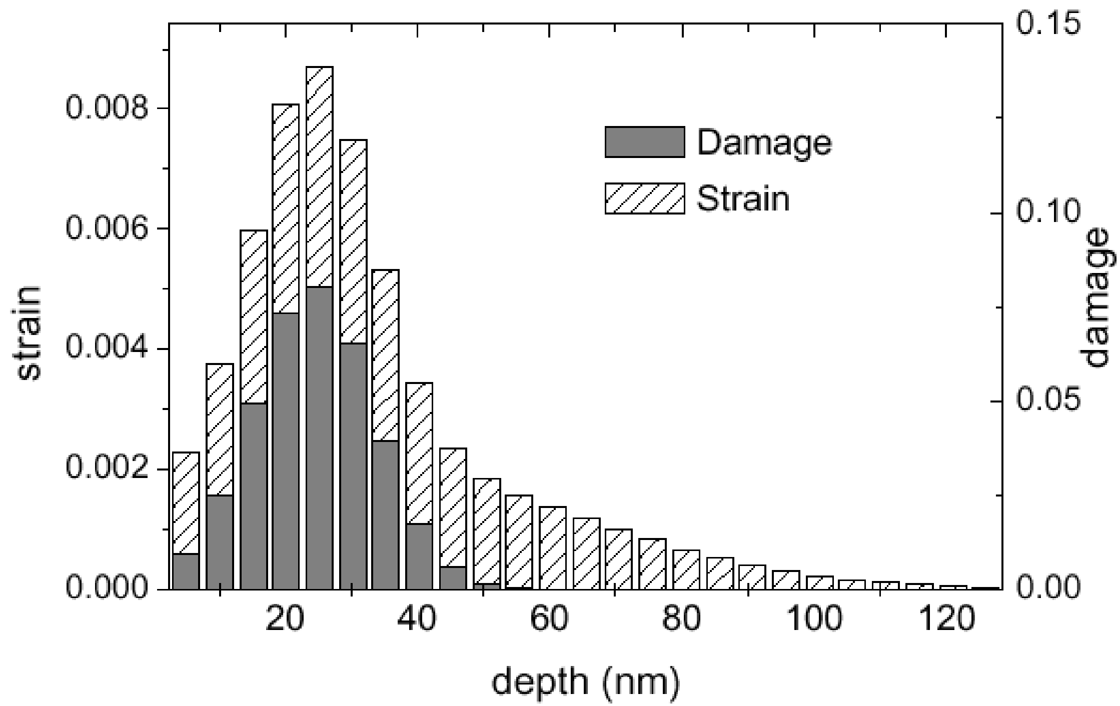

Figure 7: Cohen et al.

Fig. 7. Strain and damage profile determined from the simulation of the SOI layer implanted with a Ge dose of $3x10^{13}$ cm^{-2} and energy of 50 keV.

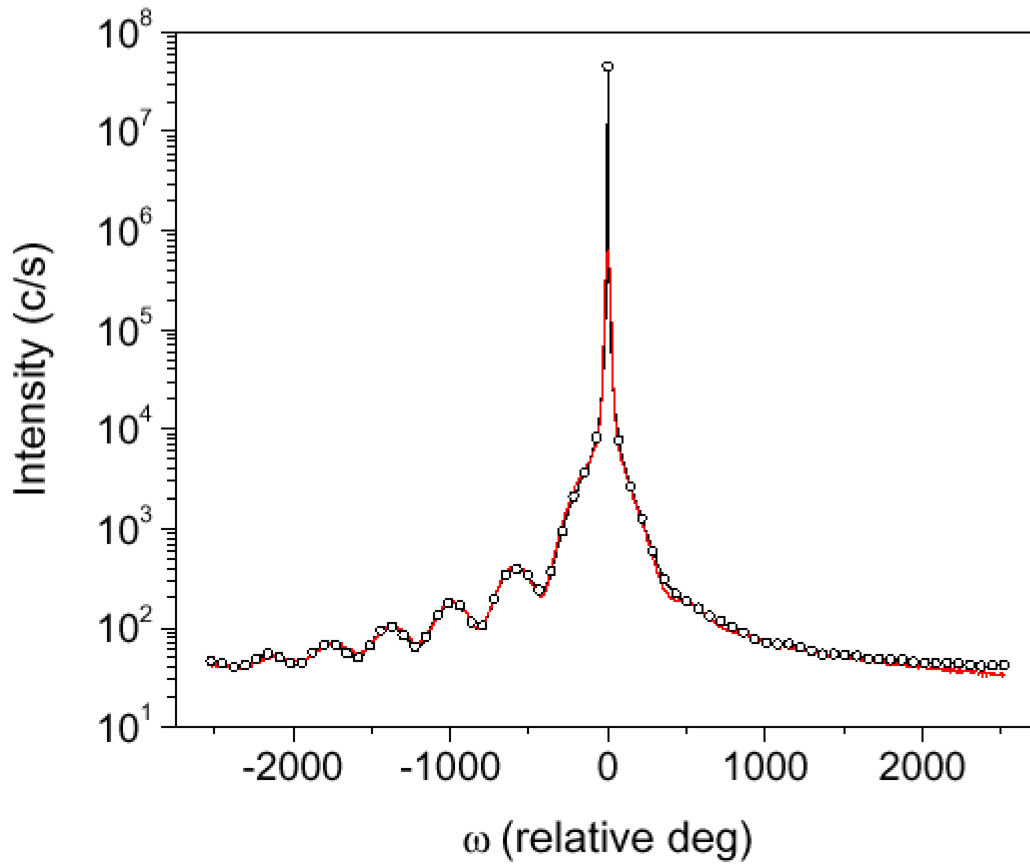

Figure 8: Cohen et al.

Fig. 8. The measured (solid line) and simulated (open circles) 113 rocking curves of an SOI film implanted with an amorphizing Ge dose of $3x10^{14}$ cm^{-2} and energy of 30 keV. A TEM cross-section of this sample is shown in Fig.4(c). The thickness of the crystalline portion of the SOI film obtained from simulation is 86 nm.

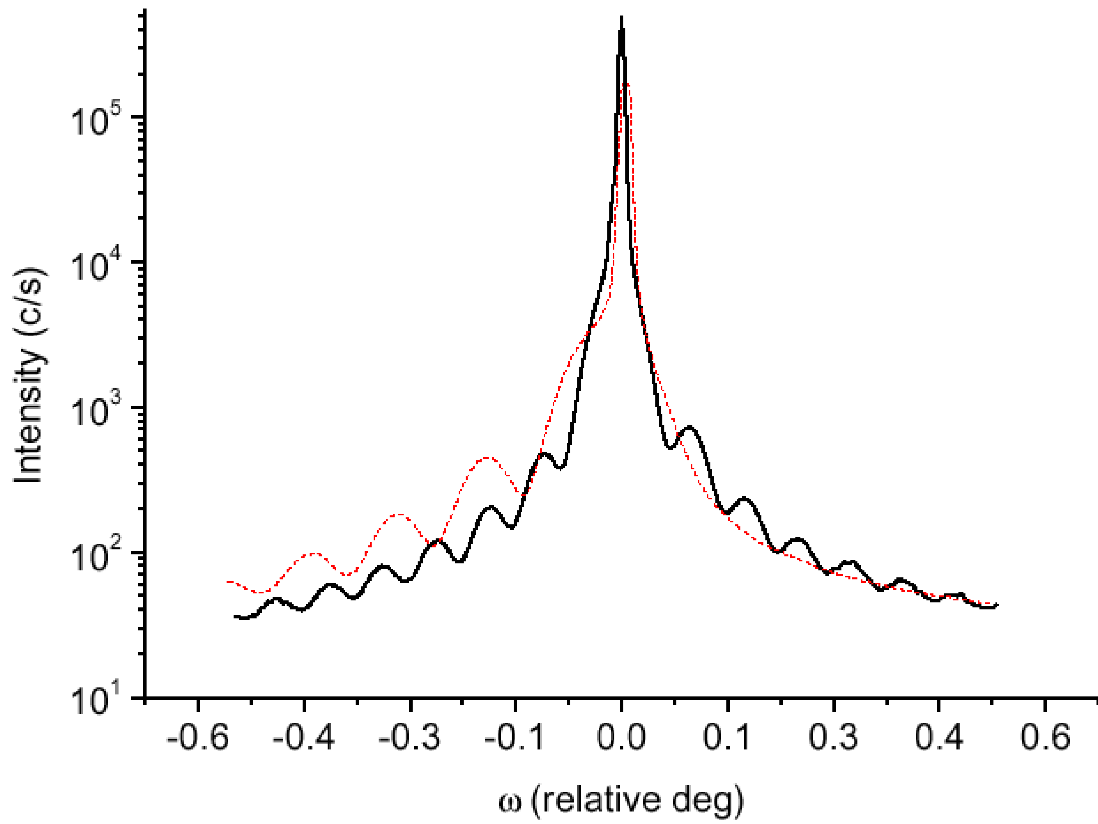

Fig. 9. 113 rocking curves of a SIMOX sample that was implanted with a Si dose of $5x10^{14}$ cm^{-2} and energy of 23.8 keV (dashed line) and then annealed at 1000 °C for 2 seconds by RTA (solid line).

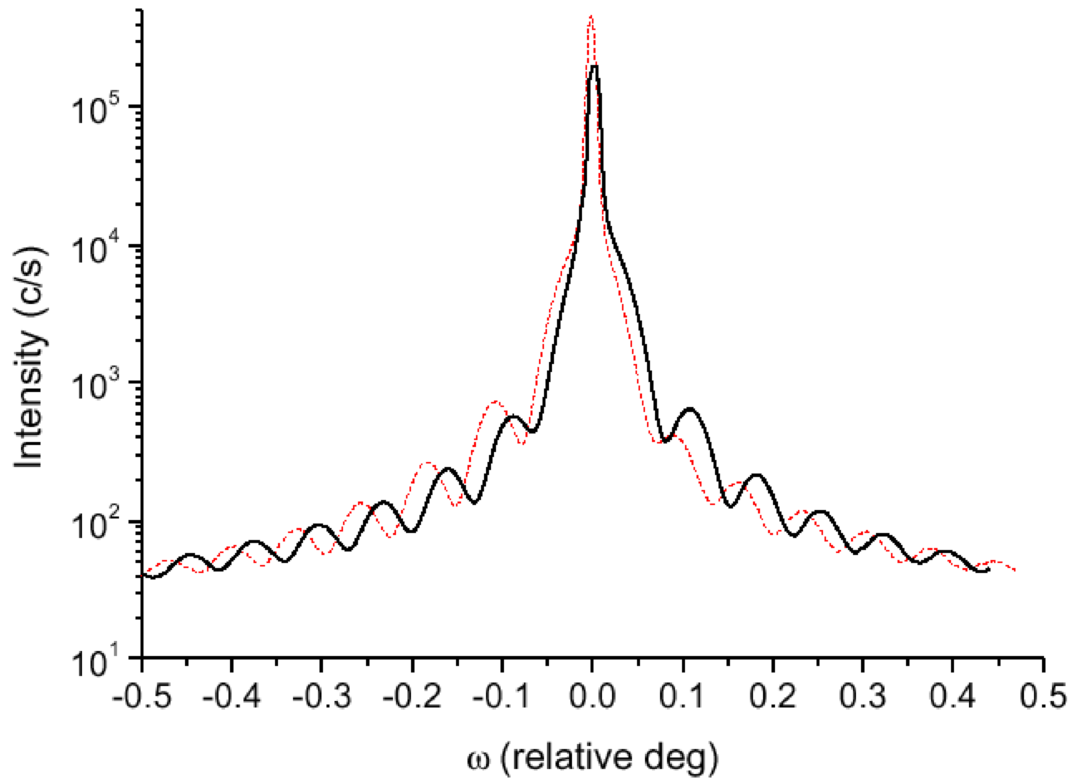

Figure 10: Cohen et al.

Fig. 10. 113 rocking curves of a sample that was implanted with a boron dose of $3x10^{14}$ cm^{-2} and energy of 3.8 keV (dashed line) and then annealed at 1000 °C for 2 seconds by RTA (solid line).